SUPPLEMENTARY FIGURE LEGENDS

Supplementary Figure S1. Fluorescence recovery after photobleaching of EGFP-UAP56, EGFP-ALY/REF and EGFP-NXF1. These are representative cells from Figure 1. HeLa cells were transiently transfected with EGFP-fusion proteins. After 48 hours, cells were treated with AKT inhibitor (5μM) before photobleaching. Control cells were treated without the drug. The same cell is shown before photobleaching, just after photobleaching, and when the recovery has reached a plateau. The bleach zone for each cell is indicated by the white square. Size bar = 5μm.

Supplementary Figure S2. The drugs used in FRAP studies inhibit PI3 kinase, AKT and mTOR activation. HeLa cells were treated as in FRAP experiments treated for 4 hours with LY294002 (20 μM), AKT inhibitor (5μM) or Rapamycin (100nM). Cellular lysates were analyzed by Western blot probed with primary antibodies specific for mTOR, for the phosphorylated serine-2448 epitope of activated mTOR, for AKT, or for the phosphorylated threonine-308 epitope of activated AKT. The loading control, actin, was detected with a mouse monoclonal antibody. Secondary anti-rabbit or anti-mouse horseradish peroxidase conjugated antibodies were developed with the SuperSignal West Pico Chemiluminescent Substrate (Pierce, Rockford, IL).

Supplementary Figure S3. Fluorescence recovery after photobleaching of EGFP-eIF4A3, EGFP-MAGOH and EGFP-Y14. These are representative cells from Figure 3. HeLa cells were transiently transfected with EGFP-fusion proteins. After 48 hours, cells were treated with AKT inhibitor (5μM) before photobleaching. Control cells were treated without the drug. The same cell is shown before photobleaching, just after photobleaching, and when the recovery has reached a plateau. The bleach zone for each cell is indicated by the white square. Size bar = 5μm.

Supplementary Figure S4. Inhibition of PI3 kinase, AKT, and mTOR had modest effects on the total content of selected mRNAs. These effects did not correlate with

the effects on nuclear to cytoplasmic partitioning measured for individual transcripts (compare with Figure 6) or with bulk poly(A) RNA (compare with Figure 4). Cells were treated with LY294002 (20μM), AKT inhibitor VIII (5μM) and Rapamycin (100nM), or were untreated, for 4 hours at 37^{o}C. Endogenous mRNAs from unfractionated cells in the same experiments as shown in Fig. 6 were quantified by qRT-PCR . As in Figure 6, Ct values were normalized using the mini UAA1 mRNA internal standard before RNA isolation. Each point represents the mean of two independent experiments in which triplicates were analyzed. Error bars represent the standard error of the mean. ns = not significant.

Supplementary Figure S5. AKT inhibition increased the amount of GAPDH intron-containing mRNA in the cytoplasm. The inhibition of AKT does increase the level of intron-containing GAPDH transcripts in the cytoplasm, consistent with a premature release from the nucleus. The effect, however, was very small and intron-containing transcripts make only a small fraction of the increase in cytoplasmic mRNA after drug treatment. Cells were treated with AKT inhibitor VIII (5 μM) for 4 hours before separation of nuclear and cytoplasmic RNA. Two sets of primers were used for qRT-PCR, one to detect intron 7 and the other to detect the exon7-intron7 junction of the GAPDH pre-mRNA. qPCR has been done using purified RNAs from nuclear and cytoplasmic fractions. Ct values were normalized using mini UAA1 mRNA from yeast added as an internal standard to each fraction after the separation of nuclei and cytoplasm. Each point represents the mean of two independent experiments in which triplicates were analyzed. Error bars represent the standard error of the mean. P≤0.01 = **; ns = not significant.

Supplementary Figure S6. The PI3 kinase, AKT, and mTOR signaling pathways do not change the degradation rate of selected mRNAs. HeLa cells were plated in 6-well plates and, after 48 hours, treated with Actinomycin D (+ActD) at final concentration of 0.5μg/ml for 7 hours. Over the last 3 hours cells were also treated with the drugs: LY294402 (20μM), AKT inhibitor VIII (5μM) and Rapamycin (100nM). Endogenous mRNAs from unfractionated cells were isolated and quantified by qRT-PCR. Ct values

were normalized using the mini UAA1 mRNA internal standard before RNA isolation. Data are expressed as fold change relative to the sample untreated without Actinomycin D (-ActD). Each point is the mean of two independent experiments in which triplicates were analyzed. Error bars are the standard errors of the mean.

Supplementary Figure S7. The PI3 kinase, AKT, and mTOR signaling pathways have transcript-specific effects on transcription rates that cannot account for the decreased nuclear to cytoplasmic partitioning after AKT inhibition. HeLa cells were plated in 6-well plates and, after 48 hours, treated with DRB (100mM) for 7 hours. Over the last 3 hours cells were then treated with the drugs LY294402 (20μM), AKT inhibitor VIII (5μM) and Rapamycin (100nM). After this period, fresh medium lacking DRB was added to resume transcription. Cells were then harvested after 0, 15 and 30 minutes. Endogenous pre-mRNAs from unfractionated cells were isolated and quantified by qRT-PCR using intron-exon primer pairs to selectively measure unsliced mRNA. Ct values were normalized using the mini UAA1 mRNA internal standard before RNA isolation. Data are expressed as fold changes relative to each treatment at minute 0 of the chase. Each point represents the mean of two independent experiments in which triplicates were analyzed. Error bars represent the standard error of the mean.

SUPPLEMENTARY MOVIES

Movie 1. Fluorescence recovery of EGFP-UAP56. HeLa cells transiently expressing EGFP-UAP56 were imaged by confocal laser scanning microscopy. EGFP-UAP56, concentrated at a RNA spicing nuclear speckled domain, was photobleached (white square). After bleaching, single images were acquired every 6 seconds for 115 seconds. This movie is from one of the cells analyzed in Figure 1

Movie 2. Fluorescence recovery of EGFP-ALY/REF. HeLa cells transiently expressing EGFP-ALY/REF were imaged by confocal laser scanning microscopy. A region containing nucleoplasm and few RNA splicing speckled domains was

photobleached (white square). After bleaching, single images were acquired every 6 seconds for 85 seconds. This movie is from one of the cells analyzed in Figure 1

Movie 3. Fluorescence recovery of EGFP-NXF1. HeLa cells transiently expressing EGFP-NXF1 were imaged by confocal laser scanning microscopy. A region containing EGFP-NXF1 was bleached (white square) and the fluorescence recovery of that region was measured. After bleaching, single images were acquired every 6 seconds for 85 seconds. This movie is from one of the cells analyzed in Figure 1

Movie 4. Fluorescence recovery of EGFP-eIF4A3. HeLa cells transiently expressing EGFP-eIF4A3 were imaged by confocal laser scanning microscopy. EGFP-eIF4A3, concentrated at a single RNA solicing speckled domain, was bleached (white square). After bleaching, single images were acquired every 6 seconds for 85 seconds. This movie is from one of the cells analyzed in Figure 2

M**ovie 5. Fluorescence recovery of EGFP-MAGOH.** HeLa cells transiently expressing EGFP-MAGOH were imaged by confocal laser scanning microscopy. The EGFP-MAGOH concentrated at a single RNA splicing speckled domain was bleached (white square). After bleaching, single images were acquired every 6 seconds for 85 seconds. This movie is from one of the cells analyzed in Figure 2.

Movie 6. Fluorescence recovery of EGFP-Y14. HeLa cells transiently expressing EGFP-Y14 were imaged by confocal laser scanning microscopy. The EGFP-eIFY14 concentrated at a single RNA splicing speckled domain, was bleached (white square). After bleaching, single images were acquired every 6 seconds for 85 seconds. This movie is from one of the cells analyzed in Figure 2.

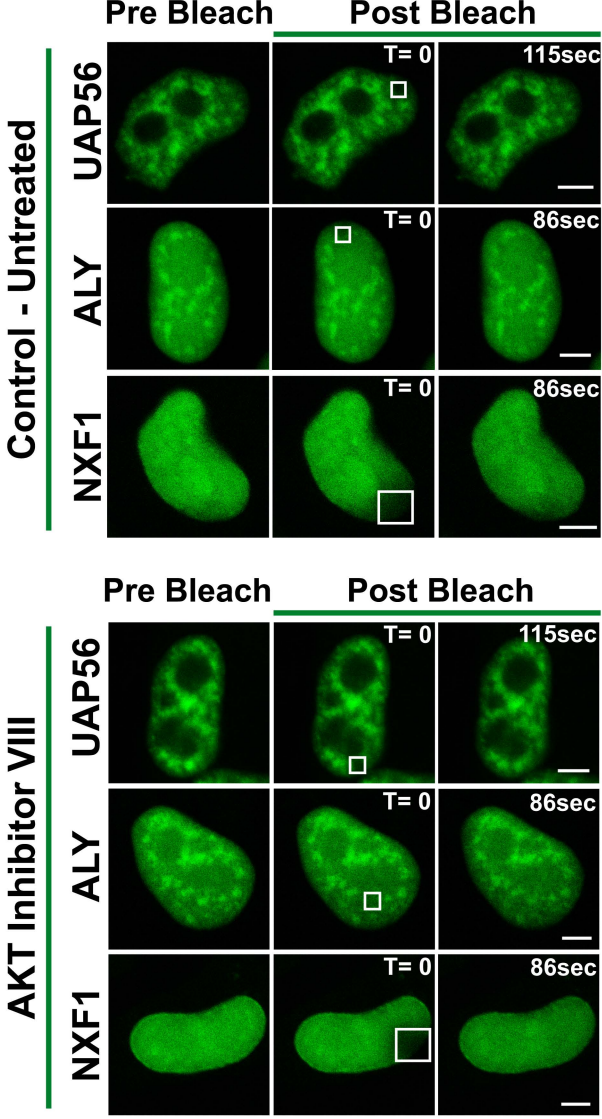

Supplementary Figure S1. Fluorescence recovery after photobleaching of EGFP-UAP56, EGFP-ALY/REF and EGFP-NXF1. These are representative cells from Figure 1. HeLa cells were transiently transfected with EGFP-fusion proteins. After 48 hours, cells were treated with AKT inhibitor (5μM) before photobleaching. Control cells were treated without the drug. The same cell is shown before photobleaching, just after photobleaching, and when the recovery has reached a plateau. The bleach zone for each cell is indicated by the white square. Size bar = 5μm.

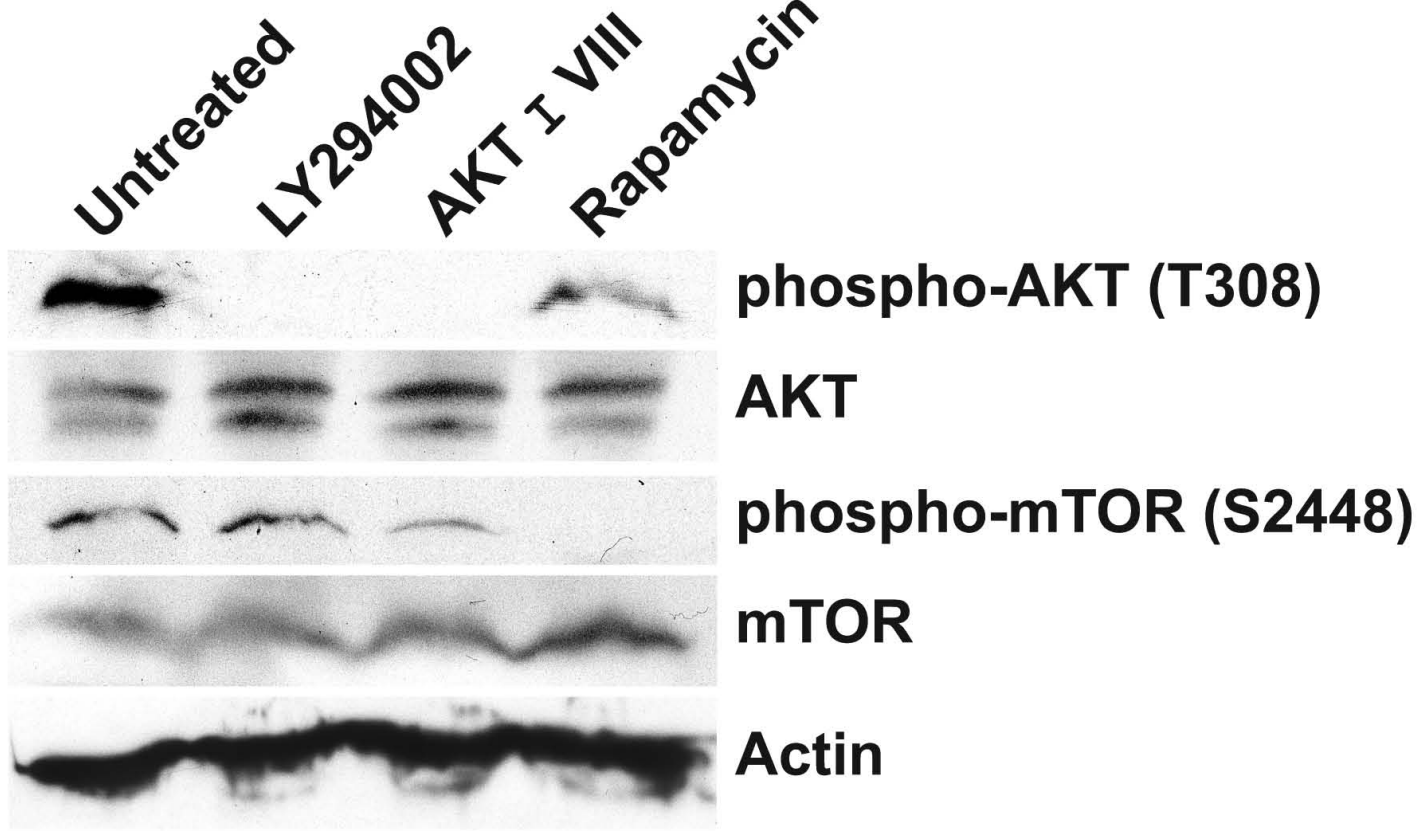

Supplementary Figure S2. The drugs used in FRAP studies inhibit PI3 kinase, AKT and mTOR activation. HeLa cells were treated as in FRAP experiments treated for 4 hours with LY294002 (20 μM), AKT inhibitor (5μM) or Rapamycin (100nM). Cellular lysates were analyzed by Western blot probed with primary antibodies specific for mTOR, for the phosphorylated serine-2448 epitope of activated mTOR, for AKT, or for the phosphorylated threonine-308 epitope of activated AKT. The loading control, actin, was detected with a mouse monoclonal antibody. Secondary anti-rabbit or anti-mouse horseradish peroxidase conjugated antibodies were developed with the SuperSignal West Pico Chemiluminescent Substrate (Pierce, Rockford, IL).

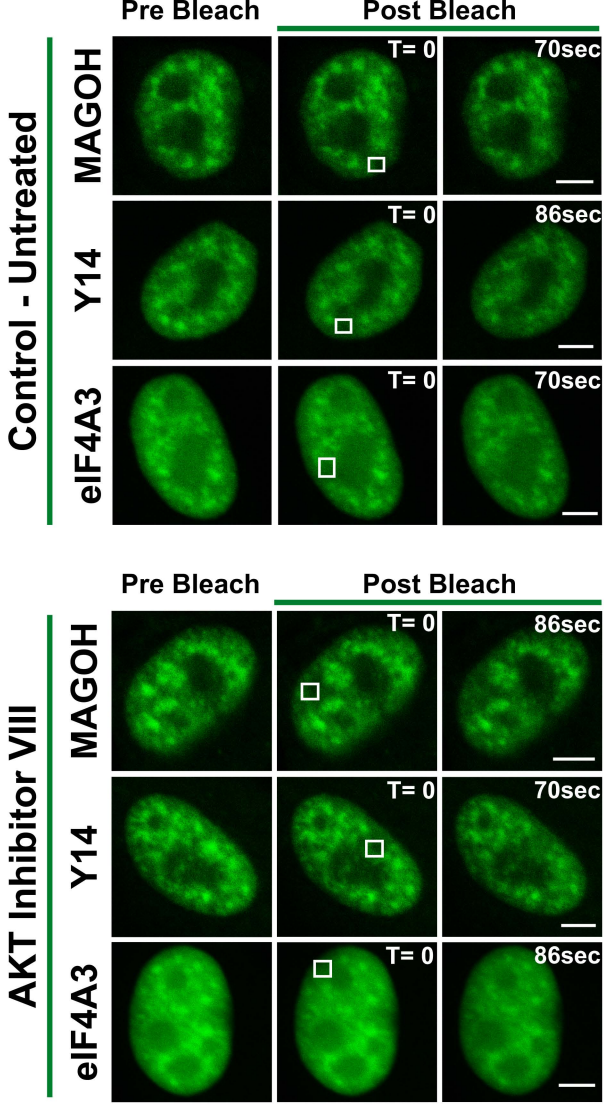

Supplementary Figure S3. Fluorescence recovery after photobleaching of EGFP-eIF4A3, EGFP-MAGOH and EGFP-Y14. These are representative cells from Figure 3. HeLa cells were transiently transfected with EGFP-fusion proteins. After 48 hours, cells were treated with AKT inhibitor (5μM) before photobleaching. Control cells were treated without the drug. The same cell is shown before photobleaching, just after photobleaching, and when the recovery has reached a plateau. The bleach zone for each cell is indicated by the white square. Size bar = 5μm.

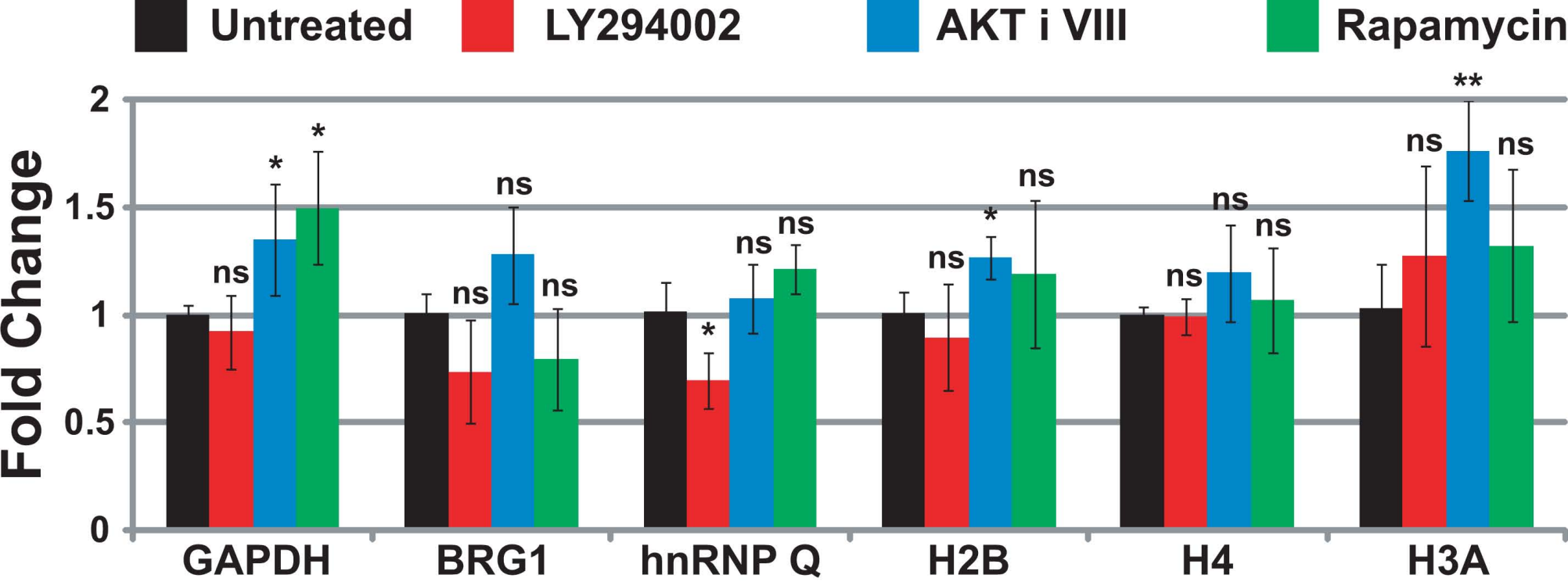

Supplementary Figure S4. Inhibition of PI3 kinase, AKT, and mTOR had modest effects on the total content of selected mRNAs. These effects did not correlate with the effects on nuclear to cytoplasmic partitioning measured for individual transcripts (compare with Figure 6) or with bulk poly(A) RNA (compare with Figure 4). Cells were treated with LY294002 (20μM), AKT inhibitor VIII (5μM) and Rapamycin (100nM), or were untreatedfor 4 hours at 37oC. Endogenous mRNAs from unfractionated cells in the same experiments as shown in Figure 6 were quantified by qRT-PCR . As in Figure 6, Ct values were normalized using the mini UAA1 mRNA internal standard before RNA isolation. Each point represents the mean of two independent experiments in which triplicates were analyzed. Error bars represent the standard error of the mean. ns = not significant.

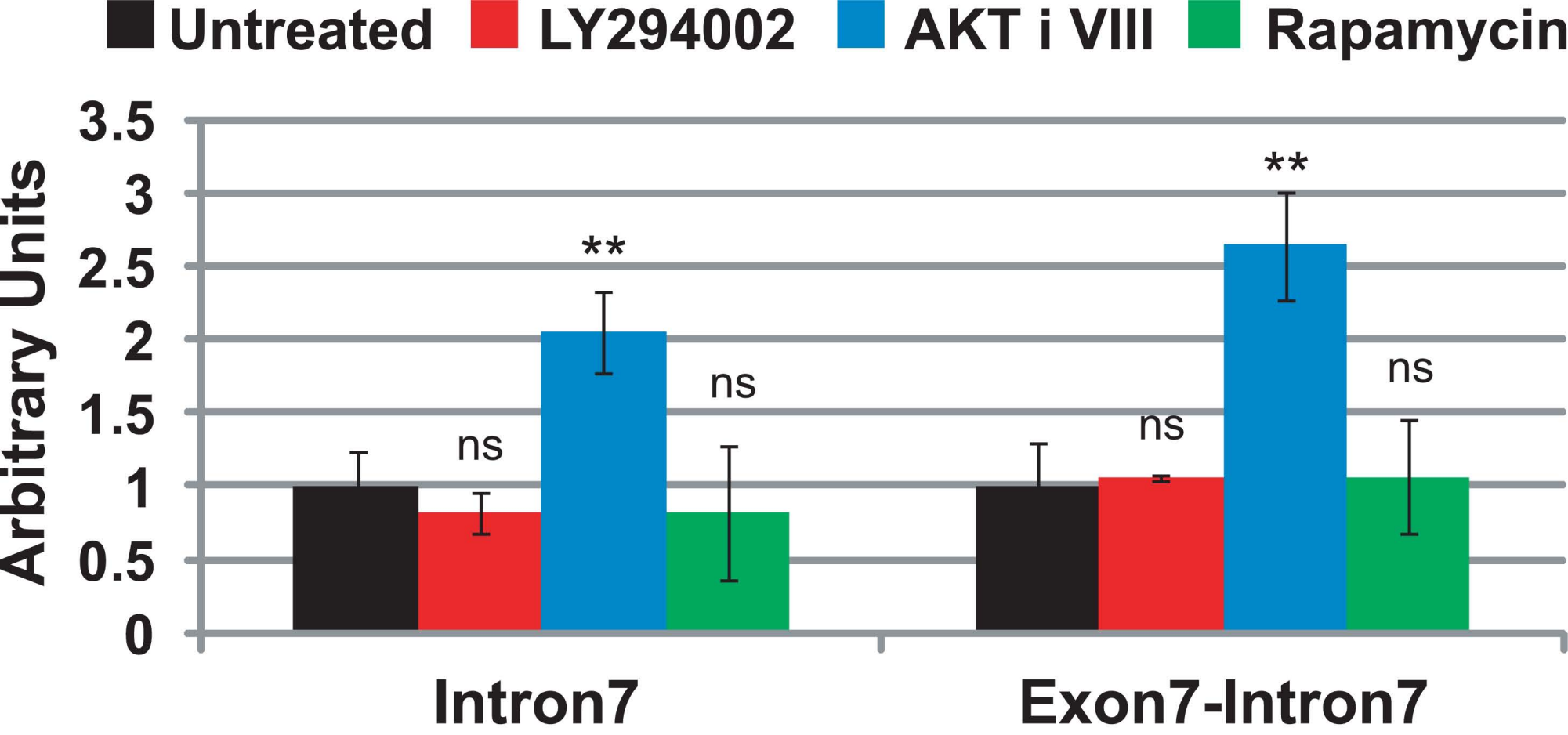

Supplementary Figure S5. AKT inhibition increased the amount of GAPDH intron-containing mRNA in the cytoplasm. The inhibition of AKT does increase the level of intron-containing GAPDH transcripts in the cytoplasm, consistent with a premature release from the nucleus. The effect, however, was very small and intron-containing transcripts make only a small fraction of the increase in cytoplasmic mRNA after drug treatment. Cells were treated with AKT inhibitor VIII (5 μM) for 4 hours before separation of nuclear and cytoplasmic RNA. Two sets of primers were used for qRT-PCR, one to detect intron 7 and the other to detect the exon7-intron7 junction of the GAPDH pre-mRNA. qPCR has been done using purified RNAs from nuclear and cytoplasmic fractions. Ct values were normalized using mini UAA1 mRNA from yeast added as an internal standard to each fraction after the separation of nuclei and cytoplasm. Each point represents the mean of two independent experiments in which triplicates were analyzed. Error bars represent the standard error of the mean.
P≤0.01 = **; ns = not significant.

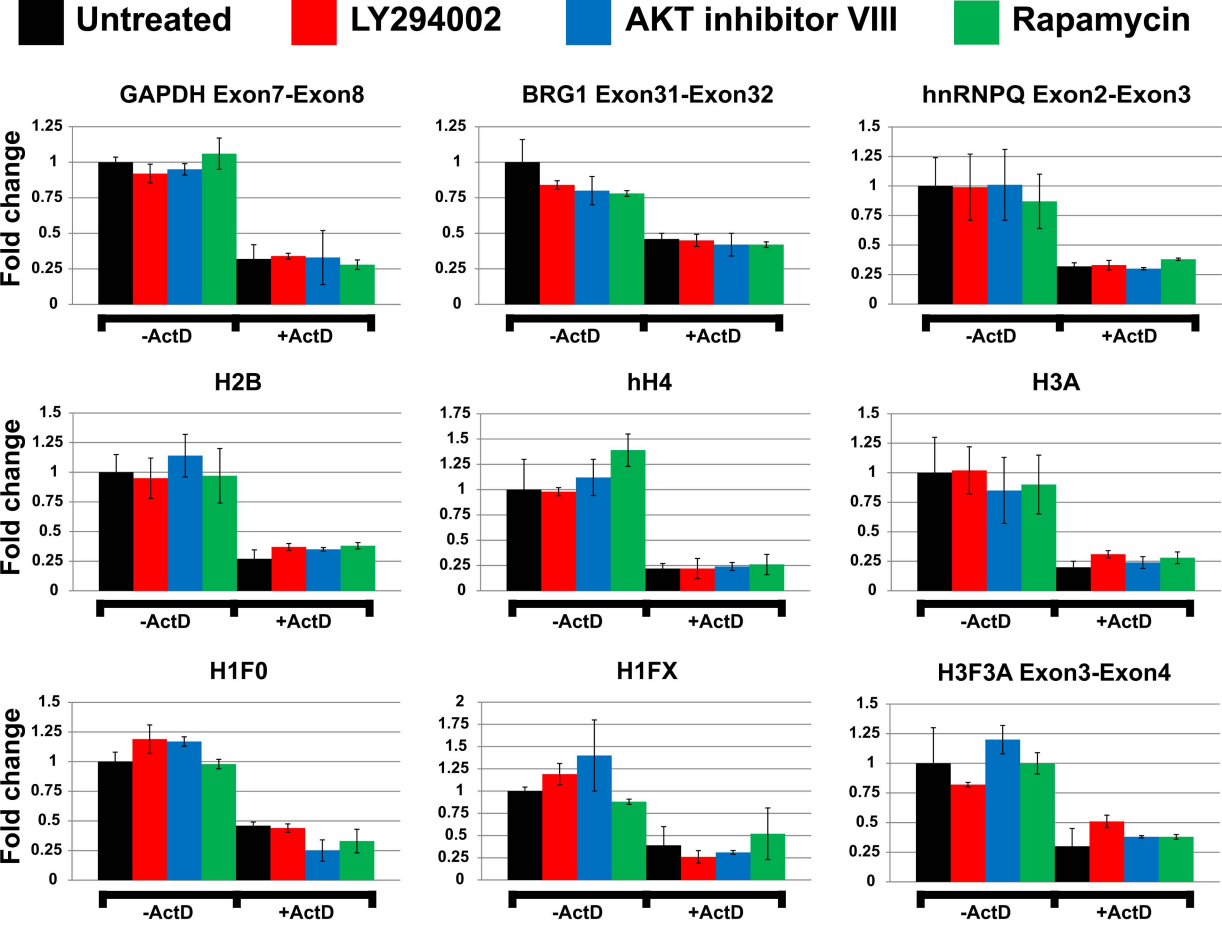

Supplementary Figure S6. The PI3 kinase, AKT, and mTOR signaling pathways do not change the degradation rate of selected mRNAs. HeLa cells were plated in 6-well plates and, after 48 hours, treated with Actinomycin D (+ActD) at final concentration of 0.5μg/ml for 7 hours. Over the last 3 hours cells were also treated with the drugs: LY294402 (20μM), AKT inhibitor VIII (5μM) and Rapamycin (100nM). Endogenous mRNAs from unfractionated cells were isolated and quantified by qRT-PCR. Ct values were normalized using the mini UAA1 mRNA internal standard before RNA isolation. Data are expressed as fold change relative to the sample untreated without Actinomycin D (-ActD). Each point is the mean of two independent experiments in which triplicates were analyzed. Error bars are the standard errors of the mean.

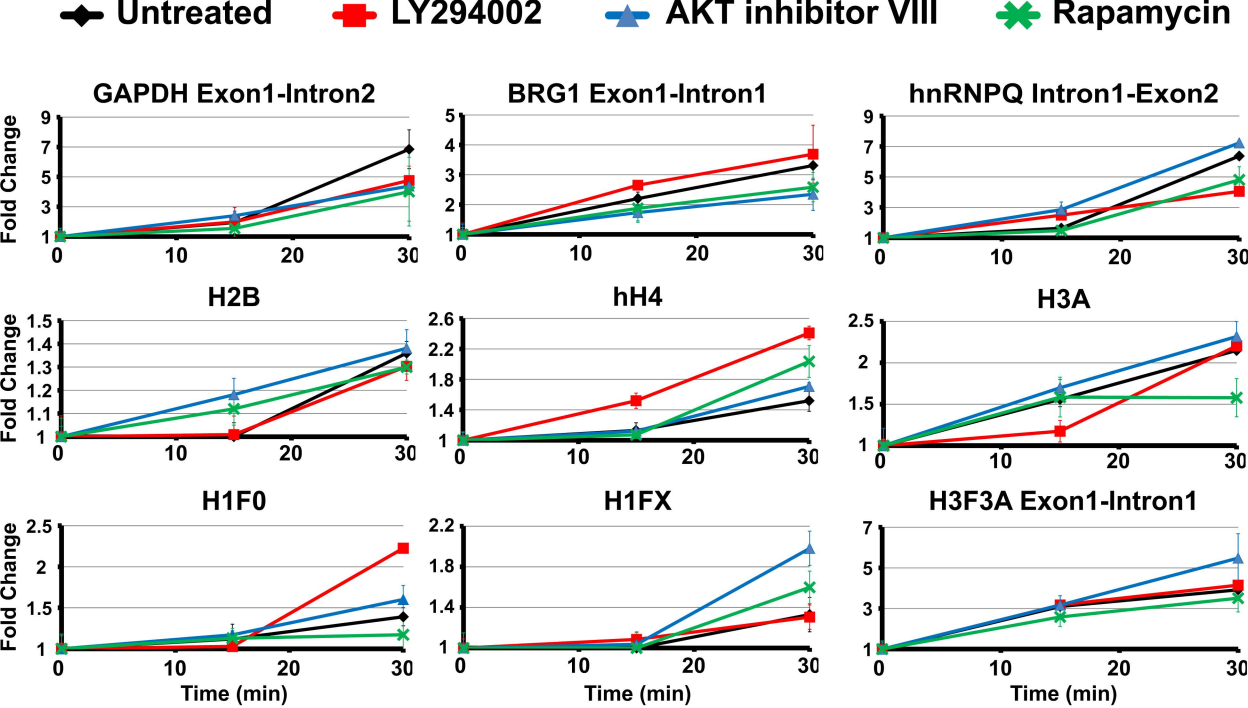

Supplementary Figure S7. The PI3 kinase, AKT, and mTOR signaling pathways have transcript-specific effects on transcription rates that cannot account for the decreased nuclear to cytoplasmic partitioning after AKT inhibition. HeLa cells were plated in 6-well plates and, after 48 hours, treated with DRB (100μM) for 7 hours. Over the last 3 hours cells were then treated with the drugs LY294402 (20μM), AKT inhibitor VIII (5μM) and Rapamycin (100nM). After this period, fresh medium lacking DRB was added to resume transcription. Cells were then harvested after 0, 15 and 30 minutes. Endogenous pre-mRNAs from unfractionated cells were isolated and quantified by qRT-PCR using intron-exon primer pairs to selectively measure unsliced mRNA. Ct values were normalized using the mini UAA1 mRNA internal standard before RNA isolation. Data are expressed as fold changes relative to each treatment at minute 0 of the chase. Each point represents the mean of two independent experiments in which triplicates were analyzed. Error bars represent the standard error of the mean.